Challenging Glass 6 - Conference on Architectural and Structural Applications of Glass
Louter, Bos, Belis, Veer, Nijsse (Eds.), Delft University of Technology, May 2018.

ISBN 978-94-6366-044-0, https://doi.org/10.7480/cgc.6.2205

Experimental Investigation on the Impact Resistance of Laminated Glass with Various Glass Make-ups

Xing-er Wang [a], Jian Yang [a, b], Han Xu [a]
[a] *School of Naval Architecture, Ocean and Civil Engineering, Shanghai Jiao Tong University, China*
[b] *School of Civil Engineering, University of Birmingham, UK*

Laboratory testing data concerning the full sized laminated glass panel with different glass make-ups under impact is limited. An experimental investigation on the impact resistance of LG panels under hard body impact is reported in this paper. A test approach namely, mean minimum breakage velocity approach, is adopted to capture the minimum impact energy that triggers each glass breakage. The crack morphology of glass panels is firstly investigated. Results indicate that the intersection angle of the radial crack edges increases when the strengthening level of glass decreases. The impact resistance is then revealed by investigating the effects caused by three design variables, i.e., the glass types, interlayer thickness and interlayer types. It reveals that the configuration with inner HS glass and outer FT glass panel can provide better impact resistance, and performs better in keeping initial stiffness under repeated impacts with higher impact velocity. In the contrast, placing HS glass in the both side may weaken the impact resistance. A 1.52 mm PVB interlayer can provide better impact resistance and higher initial stiffness when compared to a thicker interlayer, it is more likely to produce stiffness degradation between consecutive breakages as well. The difference of SGP LG and PVB LG in MMBV is found to be negligible, however, SGP LG exhibits evidently higher initial pre breakage stiffness and remains greater post breakage strength.

Keywords: Laminated glass; Impact fracture; Laboratory test; Dynamic load;

1. Introduction

The use of Polyvinyl butyral (PVB) interlayer has dominated the manufacturing of laminated glass (LG) in the last few decades. Acting as load bearing elements of novel glass structures, laminated glass comprising SentryGlas®Plus (SGP) (Bennison et al. 2002) polymer which has higher stiffness and strength, is also increasingly adopted in the construction sector. However, the brittle failure of glass panel leads to significant vulnerability of laminated glass under dynamic loading such as windborne debris impact (Kaiser et al. 2000) in the hurricane, and head impact (Rooij et al. 2003) in car accidents.

Following the specifications introduced by ASTM E1886 (ASTM E1886-13a, Standard Test Method for Performance of Exterior Windows, Curtain Walls, Doors, and Impact Protective Systems Impacted by Missile(s) and Exposed to Cyclic Pressure Differentials 2013) and E1996 (ASTM E1996-14a, Standard Specification for Performance of Exterior Windows, Curtain Walls, Doors, and Impact Protective Systems Impacted by Windborne Debris in Hurricanes 2014), small size steel balls (Knight et al. 1977; Pantelidesa et al. 1992) and large size lumbers (Zhang et al. 2013) have been chosen by several researchers to represent windborne hard and soft projectiles, respectively. 0.2 × 0.2 m laminated glass panels consisting of annealed (AN) glass layers were tested using 1.8 - 2.2 gram granite chipping with an impact velocity in the range of 4 - 20 $m \cdot s^{-1}$ (Grant et al. 1998), and the critical velocities for damage initiation in the outer glass layers were recorded. Large scale tests of laminated glass under impact of small missiles weighing 2 to 28.2 gram were conducted, in which glass sized 1.52 m × 1.83 m and 0.61 m × 0.61 m were used (Saxe et al. 2002). A mean minimum breakage velocity (MMBV) for breaking the inner glass layer was determined. Zhang (Zhang et al. 2013) tested annealed glass windows under large size lumber impact in an impact velocity range from 9 $m \cdot s^{-1}$ to 35 $m \cdot s^{-1}$. The effects of interlayer thickness on the penetration resistance and the vulnerability of LG windows with various thicknesses and dimensions were discussed.

The impactor in car accidents is commonly the pedestrian head. Liu (Liu et al. 2016) carried out a set of tests on real car windscreens under headform impact at impact angles ranging from 60° to 90°. The evaluation of the peak contact force and head injury criterion demonstrated the correlation between the PVB interlayer properties and the energy absorption capability of the windscreen. Pyttel (Pyttel et al. 2011) conducted a series of headform impact tests with both curved and plane laminated glass, in which the impact velocity was set from 5 $m \cdot s^{-1}$ to 12 $m \cdot s^{-1}$. A failure criterion based on the concept of critical energy threshold was then proposed for finite element simulations.

However, laboratory works that have been reported usually test laminated glass configurations with all glass panels using same glass type, without considering enough combination of glass types. The purpose of this work is to study experimentally the effects caused by design variables such as glass types, interlayer thickness and interlayer types

on the impact resistance of laminated glass panels, which are subjected to low velocity impact from a hard impactor. The crack morphology as well as the crack initiation and propagation features are firstly investigated. The minimum impact energy triggering each glass breakage is determined by using MMBV test approach. Finally the equivalent dynamic stiffness behavior in both pre and post breakage stages is examined.

2. Experimental set up

2.1. The drop weight impact test apparatus

Windborne debris, e.g. tiles or broken glass pieces, and accidental falling objects will impart impact on laminated glass elements. Design codes suggest that a hard projectile can be modelled as a 2 g steel ball (ASTM E1996 (ASTM E1996-14a, Standard Specification for Performance of Exterior Windows, Curtain Walls, Doors, and Impact Protective Systems Impacted by Windborne Debris in Hurricanes 2014)) for windborne debris, a 2.3 kg steel ball (ASTM F3007(ASTM F3007-13, Standard Test Method for Ball Drop Impact Resistance of Laminated Architectural Flat Glass 2013)) for accidental impact and a 4.11 kg steel ball (BS EN 356 (BS EN 356 - Glass in building. Security glazing. Testing and classification of resistance against manual attack 2000)) for vandal attack. However, it presents difficulty to measure impact force using impactor in a shape of ball. In this study, the impactor was designed to be a 13.5 kg weight with a spherical head of 40 mm radius and a cylindrical body. A ring type integrated circuit piezoelectric (ICP) force sensor was installed between the head and the impactor body to measure the impact force.

Figure 1 shows the drop weight testing apparatus. A steel platform was fabricated to provide the supports for bolted connections. A high-speed camera (12,500 frames per second with a resolution of 1024 × 1024 pixels) with two spotlights was adopted to record the impact process of the specimens via a mirror placed underneath the specimen, which was suggested by Van Dam's work (Van Dam 2017) (**Fig. 1 (a)**). The high-speed camera recording was triggered when the transformed voltage from the RF1 accelerometer glued to the inner surface of the LG panel (see **Fig. 1 (b)**) exceeded the specified value (nearly 2.2 V). In order to avoid impact debonding, the RF1 was 80 mm away from the panel centre instead of being located centrally beneath the impact point. All sensors were connected to data acquisition units with multiple modules. A sampling frequency of 100 kHz was adopted during the tests.

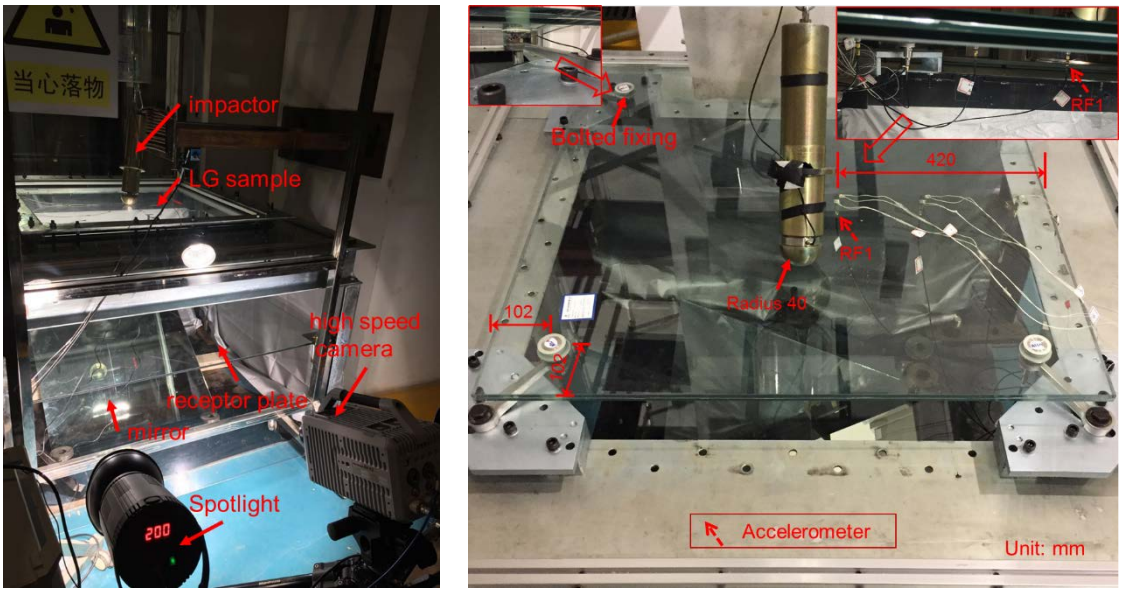

a) High speed camera set up b) Support system set up

Fig.1 The drop weight impact testing apparatus

2.2. Testing specimens

In this study, six groups of laminated glass specimens (See **Table 1**) were selected for testing. Heat strengthened (HS) and fully tempered (FT) glass were employed and combined with PVB and SGP interlayers to make different types of laminated glass. Three design variables, that were, glass type, interlayer thickness and interlayer type were taken to investigate the corresponding effects on the impact resistance of laminated glass. The specimens were 1000 mm × 1000 mm in size, with each glass panel being 8 mm thick. The interlayer thickness varied from 1.52 mm to 3.04 mm. All specimens were fixed with bolts to the testing platform using four countersunk bolts.

A mean minimum breakage velocity (MMBV) test procedure (Saxe et al. 2002) was employed in this study to capture the breakage energy that triggers the breakage of each glass panel for each type of laminated glass specimen.

The MMBV approach is characterised by a series of impact attempts with gradually increasing drop height until all glass panels break. The initial drop height between the impactor tip and the LG outer surface was based on a rough evaluation of the impact breakage energy, and each test specimen was intended to have several impact attempts before the first constituent glass panel started to break. Following the initial impact height, the drop height was increased in increments of 0.2 m. After the first constituent glass panel was broken, the drop height was reduced to a level of 0.4 m lower than that resulting in the first breakage of the glass panel. Prior to the initial impact breakage, the repeated impact attempts may generate accumulated damage on the glass surface which may not be observable. In order to investigate the influence of such damage on the elastic stiffness degradation, the specimen was tested three times at its initial drop height.

Table 1 Laminated glass configurations tested under impact

ID	LG configuration	Thickness (mm)	Support system	Dimensions (mm × mm)	Quantity	Design variable
L01	FT/PVB/FT	8/1.52/8	Bolted	1000 × 1000	6	Glass type
L02	HS/PVB/HS	8/1.52/8	Bolted	1000 × 1000	3	Glass type
L03	FT/PVB/HS	8/1.52/8	Bolted	1000 × 1000	3	Glass type
L04	HS/PVB/FT	8/1.52/8	Bolted	1000 × 1000	3	Glass type
L05	FT/PVB/FT	8/3.04/8	Bolted	1000 × 1000	3	Interlayer thickness
L06	FT/SGP/FT	8/3.04/8	Bolted	1000 × 1000	6	Interlayer type

3. Results and discussion

The breakage sequence of each specimen is classified into three categories based on experimental observations, which are: 1) BS1: outer[1]-inner[2], 2) BS2: inner[1]-outer[2] and 3) BS3: inner[1] & outer[1].

In the above category descriptions, the superscript represents the breaking order, e.g., BS3 means that both inner and outer glass layers break in the same impact. The post-breakage stage is after the first glass breakage occurs. The number of each glass configuration in different breakage sequence is recorded and listed in **Table 2**.

Table 2 The number of laminated glass specimens in various breakage sequence

ID	L01	L02	L03	L04	L05	L06
BS1	1	-	-	-	1	3
BS2	1	-	1	-	-	2
BS3	4	3	2	3	2	1

3.1. Crack morphology

The typical crack patterns observed in the experiment are rippled cracks in the outer glass panel and radial cracks in the inner glass panel. Significant differences in the local crack patterns near the impact point are observed in the different glass types. As shown in Fig. 2 (a), the outer HS glass layer exhibits a core cracked zone comprising several

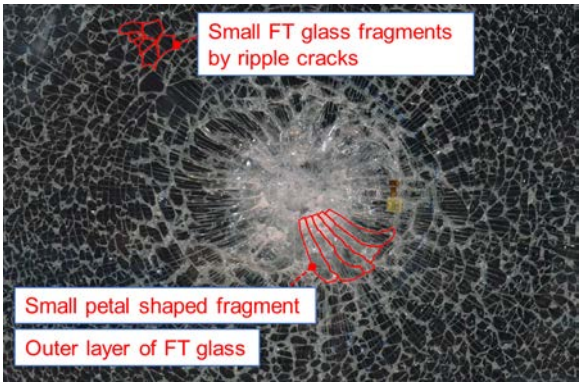

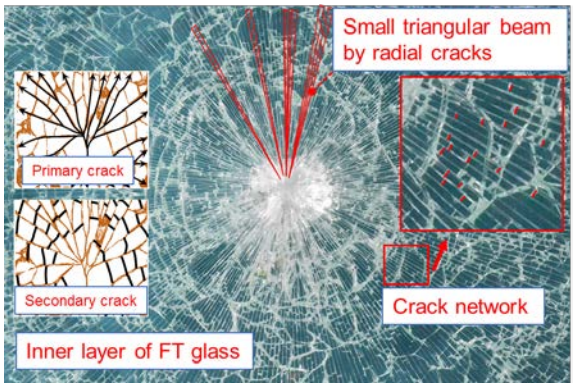

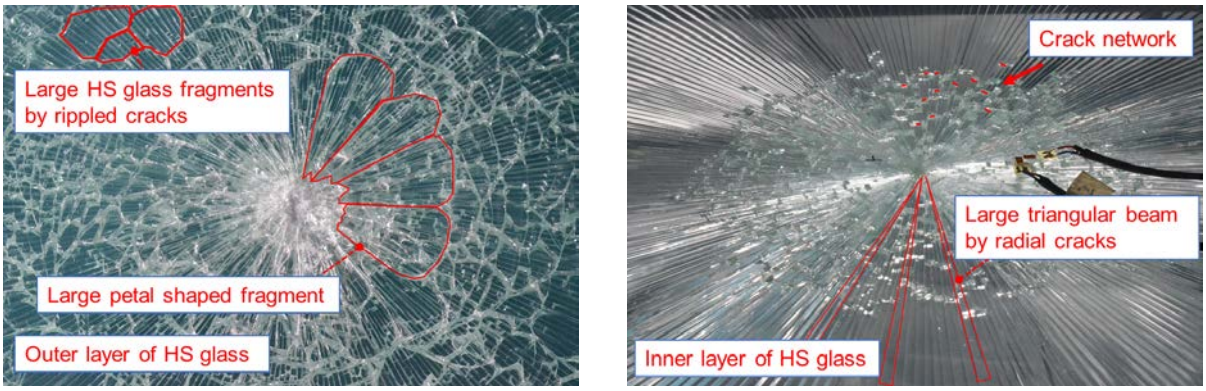

(a) Crack morphology of outer glass panel (b) Crack morphology of inner glass panel

Fig.2 Typical crack pattern of laminated glass tested

large petal shaped fragments. A circumferential crack along the edge of the petal shaped fragments can be observed and acts as a boundary dividing the core cracked zone and the rippled crack zone. Large HS glass fragments can be observed in the rippled crack zone. Likewise, the outer FT glass layer cracks into a core cracked zone with smaller petal shaped fragments, and an external rippled crack zone comprising small FT glass dices. However, the petal shaped fracture of FT glass propagates with a tendency to become skewed. This is different from the HS glass case where the outward cracks of a petal shaped fracture are almost perfectly radial with larger fragments.

In contrast, the crack morphology in the inner layer (**Fig. 2 (b)**) appears to be mostly in the radial direction and in the form of shard-shaped triangular beams. Like crack patterns that have previously been reported (Dugnani et al. 2014), the cracks in the triangular beams include: 1) primary cracks which are outgoing radial cracks, 2) secondary cracks, i.e. a crack network cutting off the different triangular beams, which is driven by the redistribution of the residual stress field. When comparing the inner HS and FT glass fragments, it can be seen that the intersection angle of the radial crack edges increases when the strengthening level of glass decreases. This leads to larger triangular beam fragments in HS glass panel.

3.2. Crack initiation and propagation

Two glass panels break in the same impact attempt in breakage sequence BS3. In order to accurately establish the breaking order of BS3, the high speed filming results were reviewed to precisely locate their crack initiation instances which were indistinguishable by the naked eye. Meanwhile, the features of their crack propagation were identified.

Fig. 3 shows the high speed photos of specimen L01-3 at impact velocity of 3.3 m/s, in which case both glass panels fracture in the same impact. Each frame of high speed photos has an interval of 0.08 ms. The radial cracks firstly initiates in the inner glass layer and reach a radius of 158 mm at 0.08 ms. Because of no cracks are observed at 0 ms, it shows that the crack propagation speed within such short duration (0.08 ms) is not less than 1975 m/s. The rippled cracks are subsequently triggered in the outer glass panel at 0.16 ms. The rippled cracks propagate outward in a manner of water wave and reach a radius of 201 mm in 0.08 ms. The initial propagation speed of rippled cracks can then be calculated to be not less than 2512 m/s. It is noting that such propagation speed (2512 m/s) is extremely fast when comparing with the data reported so far. This may be caused by the greater stress wave generated in the impact, which significantly promotes the fracturing speed of glass near impact point. When spreading to the boundary, the magnitude of stress wave will decrease rapidly because of the cushioning effects by interlayer and the reflection of stress waves. After analyzing the high speed photos after 0.16 ms, it can be seen that the propagation speed of rippled cracks decelerates to nearly 1500 m/s and agrees well with theoretical approximation (Acloque 1975) and other experimental measurements (Nielsen et al. 2008; Molnár et al. 2016).

Both radial and rippled cracks propagate to the glass panel edges at 0.40 ms, which suggests the mean crack propagation speed is approximately 1250 m/s. At 1.20 ms, the core cracked zone with petal shaped fragments continue to further fracture under the impactor motion.

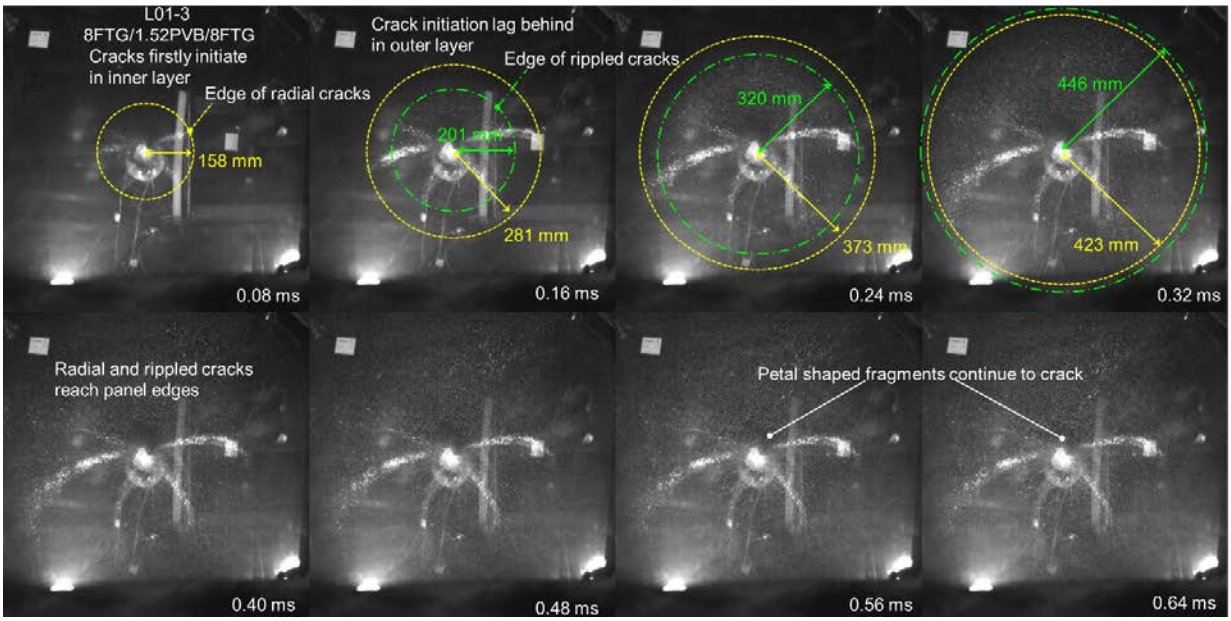

Fig. 3 Crack initiation and propagation of specimen L01-3 at impact velocity of 3.3 m/s

3.3. Breakage velocity

Breakage velocity refers to the impact velocity that triggers the breakage of each glass panel. The mean value and standard deviation of the breakage velocity v_{break} of tested specimens in different breakage sequence is shown in **Fig. 4**.

Effects of glass type:

L01 – L04 groups are laminated glass made of HS and FT glass panels with same PVB interlayer thickness of 1.52 mm. Comparing the breakage velocity of these four groups, the effects of glass type on the breakage velocity show that:

a) In breakage sequence BS2, when inner glass panel cracks, the mean breakage velocity of L03 group with inner HS glass panel has an increase of 35% than that of L01 group with inner FT glass panel. L01 and L03 achieve same breakage velocity at the second glass breakage.
b) In breakage sequence BS3, L03 group has the highest breakage velocity that is 36.7% higher than L02 group, which is made of two HS glass panels and obtains the lowest value among all groups. Comparing to L02 group, L01 group has an increase of 23% and L04 group with outer HS glass panel has a minor increase of 6.7 %.

It can be concluded that, the configuration of using inner HS glass and outer FT glass panel can evidently improve the impact resistance of laminated glass. In the contrast, it may weaken the impact resistance if HS glass is adopted in the both sides of glass panel.

Effects of interlayer thickness:

The PVB interlayer thickness varies from 1.52 mm in L01 group to 3.04 mm in L05 group. Comparing the breakage velocity of these two groups, it shows that:

a) In breakage sequence BS1, the breakage velocity of L01 group is 21% lower than the L05 group at the first breakage, while L01 and L05 groups achieve the same breakage velocity at the second breakage.
b) Only L01 group shows breakage sequence BS2, when comparing with the breakage velocity of same glass configuration of L01 in other breakage sequence, the initial breakage velocity at the first breakage in BS2 is equal to that in BS1, however, the breakage velocity at the second breakage in BS2 has a significant decrease. The results reveal that, if the inner glass panel cracks first, it will render negative effects on the remaining impact resistance of laminate glass.
c) In breakage sequence BS3, L01 group presents the greatest breakage velocity, a 22% reduction can be found in L05 group.

The comparison results show that, in most occasions, laminated glass with 1.52 mm PVB interlayer can obtain better impact resistance than that with thicker PVB interlayer. The thicker PVB interlayer can only increase the breakage velocity at the first breakage when breakage sequence BS1 occurs.

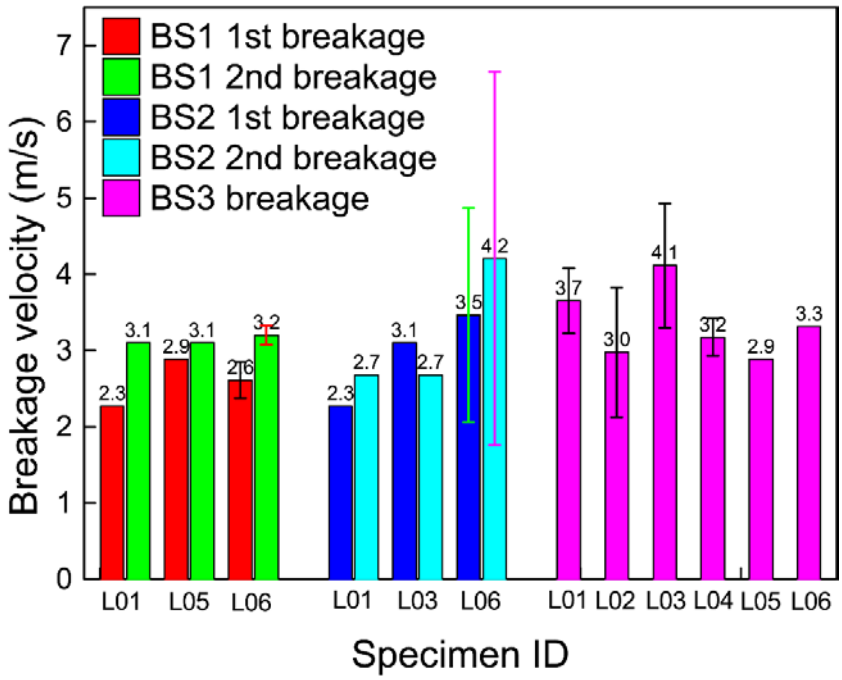

Fig. 4 Breakage velocity of laminated glass specimens in different breakage sequence

Effects of interlayer type:
The L05 and L06 groups use different interlayer types, PVB and SGP, respectively, and the interlayer is both 3.04 mm thick in these two groups. Comparing the breakage velocity of L05 and L06 groups in **Fig. 4**:

a) In breakage sequence BS1, the breakage velocity of L05 group at the first breakage has an 11.5% increase than L06 group, and presents a minor reduction at the second breakage.
b) Only L06 shows breakage sequence BS2, it can be seen that the mean breakage velocity of L06 is significantly greater than that in other breakage sequence. However, on the other hand, it has a much larger standard deviation. Such finding is caused by the different crack initiation type in one specimen of L06 group, which cracks first at the hole position at corner instead of commonly initiating in the impact point. This leads to a much greater breakage velocity of this specimen, and thus to significantly increase the mean breakage velocity. In the contrast, the breakage velocity of the other specimen in BS2 is both 2.5 m/s at ordinal breakages, which is slightly lower than that of L06 in other breakage sequence.
c) In breakage sequence BS3, L06 group has a 14% higher breakage velocity than L05 group.

The results show that, there is no significant difference of the breakage velocity between the laminated glass specimens with PVB and SGP interlayer. Despite of the minor difference in impact resistance against glass breakage, It is worth noting that the broken PVB laminated glass cannot sustain its self-weight and will continue to deform, because the PVB interlayer has failed in final impact. In contrast to such trend, the broken SGP laminated glass can still keep level and provides its partial static load capacity, showing the greater post breakage strength of SGP laminated glass.

3.4. Equivalent dynamic stiffness

During the impact attempts between two consecutive breakages, the repeated impacts may facilitate the coalescence of the microscopic flaws or cracks that cannot be seen by naked eyes. Such coalescence of microscopic cracks can be closed by the great compressive stress in the surface of thermally strengthened glass, if the impact momentum is still low. However, it may lead to a stiffness degradation when impact momentum increases and exceeds a certain value. Based on the hypothesis that the impact energy consumed by generating microscopic cracks can be negligible, the stiffness characteristics of LG panel when impact momentum increases can be evaluated by analyzing the relationship between peak impact force P_{max} and impact velocity V. The P_{max} will increase linearly with the impact velocity if no distinct stiffness degradation occurs. Here, we simply define one variable, equivalent stiffness K_{eq}, to determine the critical impact velocity that will trigger the nonlinearity of the P_{max}-V relationship.

$$K_{eq} = K_{cons}(P_{max} / V) \quad (1)$$

where V denotes the impact velocity, P_{max} represents the peak impact force, K_{cons} is a constant relating to LG panel stiffness. The peak impact force versus impact velocity of laminated glass specimens in different breakage sequence is recorded and shown in **Fig. 5**, **Fig. 6** and **Fig. 7**, respectively. Linear regression equations are used to fit the data,

the slope of the curve fitted, *K*, can be defined as equivalent dynamic stiffness. The impact velocity at the point where stiffness slope degrades can then be identified as critical velocity that determines the irreversible accumulated microscopic damage of laminated glass. It is noting that the equivalent dynamic stiffness *K* is located to trace the critical velocity and further investigate the stiffness characteristic of LG panels under repeated impacts, it is not the same concept as the traditional stiffness calculated by force and deflection.

Effects of glass type:
Comparing the equivalent dynamic stiffness of L01 - L04 groups, the effects of glass type on the dynamic stiffness can be examined, the results show that:

a) In breakage sequence BS2 (**Fig. 6**), in the pre breakage stage, equivalent stiffness *K* in L01 group with two FT glass panels is 22.3% greater than that in L03 group with inner HS glass panel. In the post breakage stage, the stiffness degradation ratio of post breakage stiffness (15.8 kN/(m·s^{-1})) to initial pre breakage stiffness (29.0 kN/(m·s^{-1})) in L01 group is approximately 54%. The post breakage stiffness cannot be obtained in L03 group because of lacking enough data.
b) In breakage sequence BS3 (**Fig. 7**), according to descending order in the initial stiffness, the specimens are sorted as following: L01, L02, L04 and L03. The initial stiffness of L01 group is highly close to L02 group, and has a 13% increase than L04 group, a 33% increase than L03 group. Stiffness degradation can be observed in all four laminated glass groups. It can be seen that the post breakage stiffness of each group is close. L03 group achieves the greatest critical velocity of 3.1 m/s. Such critical velocity is evidently higher than that of other groups, in which the critical velocity is both 2.5 m/s in L02 and L04, and 2.7 m/s in L01 group. It reveals that, although the initial stiffness of L03 group is the lowest, it is able to keep higher stiffness when subjected to repeated impacts in a larger range of impact velocity.

It can be concluded that, when compared to the configuration of adopting FT glass in both outer and inner panels, placing HS glass panel in the inner side will always result in lower initial stiffness with a similar post breakage stiffness. It also has a significant increase in critical velocity that can make laminated glass using such configuration performs better in keeping initial stiffness under repeated impacts with higher impact velocity.

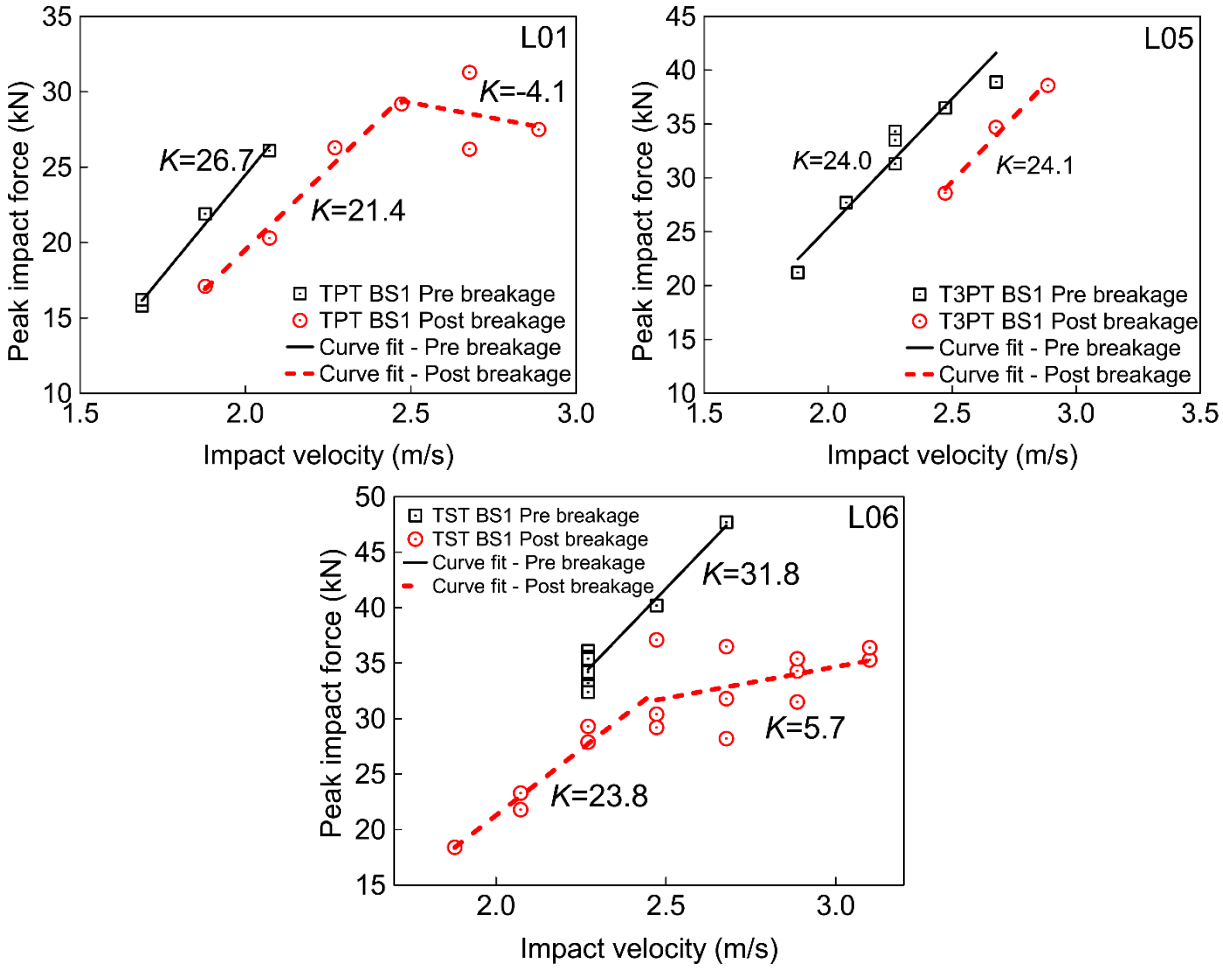

Fig. 5 Equivalent dynamic stiffness of laminated glass specimens in breakage sequence BS1

Effects of interlayer thickness:
Comparing the equivalent dynamic stiffness of L01 and L05 groups, the results demonstrate that:

a) In breakage sequence BS1 (**Fig. 5**), in the pre breakage stage, the initial stiffness of L01 group has an 11% increase than that of L05 group, showing that thicker interlayer will produce slight negative effect on pre breakage stiffness. However, in the post breakage stage, L05 group achieves 12.6% higher stiffness, indicating that the thicker interlayer can generate higher post breakage stiffness. L01 group has a remarkable stiffness degradation after reaching the critical velocity of 2.5 m/s. L05 group does not present such degradation, showing that thicker PVB interlayer can contribute to keeping reliable post breakage stiffness.
b) In breakage sequence BS3 (**Fig. 7**), the initial stiffness of L01 group has a 20% increase than that of L05 group. After the impact velocity exceeding 2.7 m/s, L01 group presents significant stiffness degradation and obtains a degraded stiffness that is nearly 41% the initial stiffness. Similar to that observed in BS1, L05 group does not show stiffness degradation as well.

The comparison result shows that the initial dynamic stiffness of laminated glass increases when reducing the interlayer thickness. However, the laminated glass with a thinner PVB interlayer is more likely to present stiffness degradation between two consecutive breakages. Such stiffness degradation ratio may be greater than 40%. Smaller critical velocity of laminated glass with thinner interlayer indicates that the glass panel will have irreversible accumulated damage much earlier.

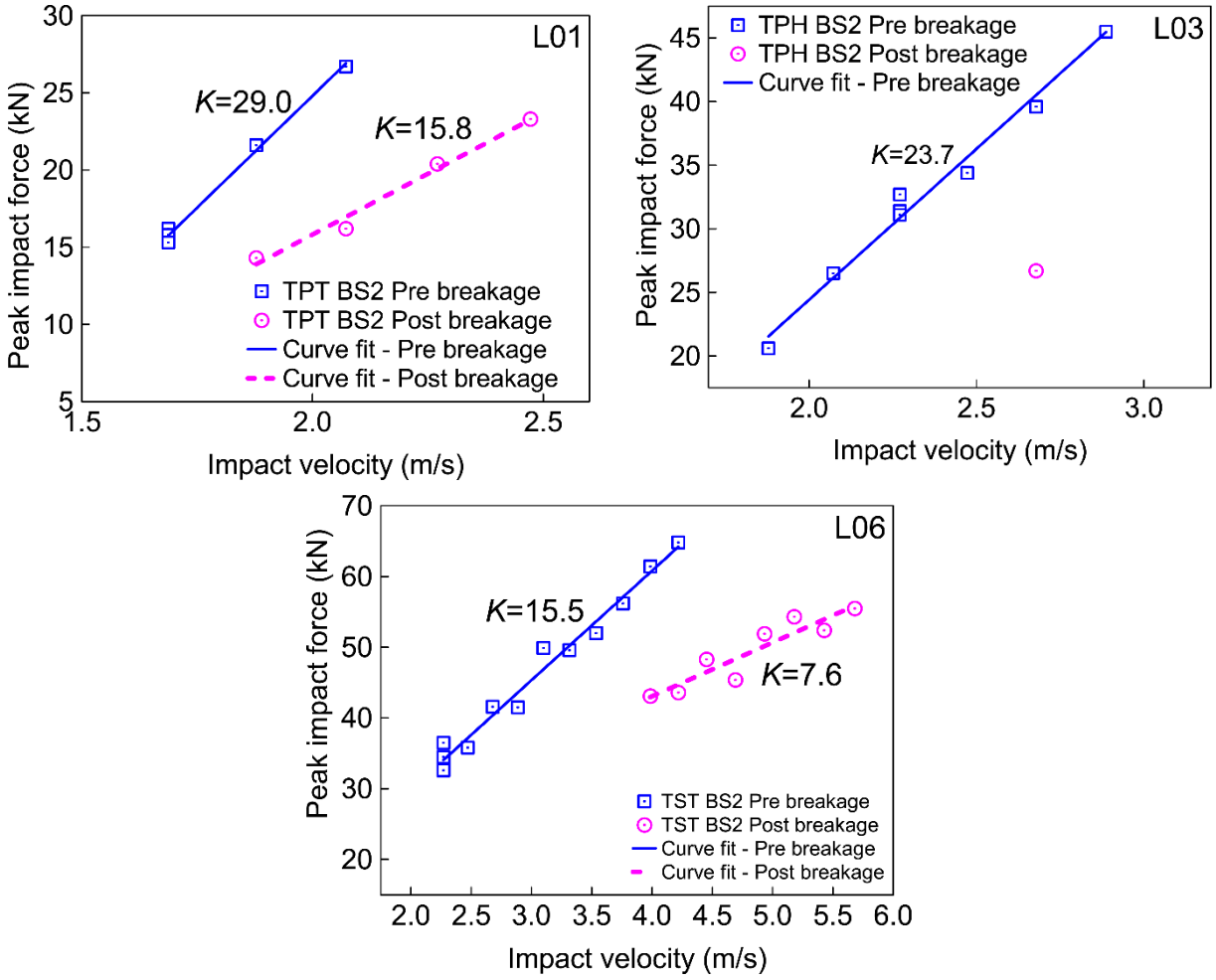

Fig. 6 Equivalent dynamic stiffness of laminated glass specimens in breakage sequence BS2

Effects of interlayer type:
Comparing the dynamic stiffness of L05 and L06 groups, it can be seen that:

a) In breakage sequence BS1 (**Fig. 5**), in the pre breakage stage, L06 group achieves higher initial stiffness than L05 group and has a remarkable increase of 32.5%. After outer glass panel cracks, the initial post breakage stiffness of L05 group is close to that of L06 group, but has no evident stiffness degradation before second breakage occurs. In the contrast, L06 group presents a stiffness degradation stage after the impact velocity exceeding 2.5 m/s, the stiffness declines to 24% the initial post breakage stiffness.

b) Only L06 presents breakage sequence BS2 (**Fig. 6**), when comparing the dynamic stiffness of L06 in BS2 with that in BS1, it can be seen that the initial stiffness in the pre breakage stage in BS2 is less than half of that in BS1, and the initial post breakage stiffness in BS2 is nearly 32% that in BS1. However, the initial pre breakage stiffness in BS1 and BS2 is predicted to be the same because no damage or fracture occurs in the early pre breakage stage, such large discrepancy may be caused by accidental installation error that leads to the weak support for the specimen cracking in BS2. It should also be noted that, the dynamic stiffness of L06 in BS3 is not available because the corresponding sensor data is found to be invalid.

It can be concluded that SGP interlayer can provide significant higher initial pre breakage stiffness than PVB interlayer with same thickness. However, such improvement does not exist in the post breakage stage, in which the laminated glass using SGP interlayer has stiffness degradation that loses nearly 75% initial post breakage stiffness after exceeding the critical velocity.

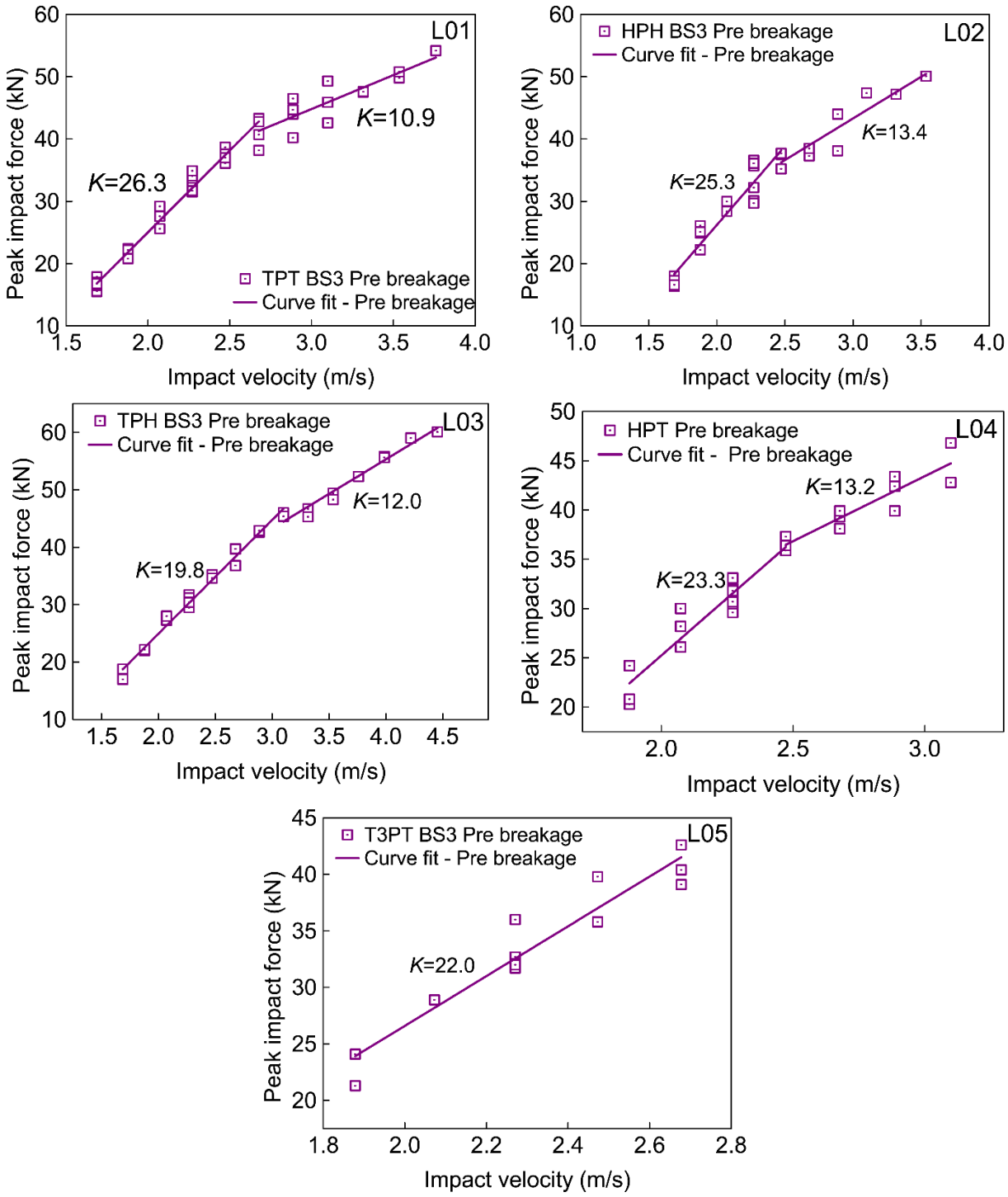

Fig. 7 Equivalent dynamic stiffness of laminated glass specimens in breakage sequence BS3

4. Conclusions

In this paper, laboratory tests were carried out to investigate the impact damage of laminated glass using various glass configurations under hard body impact. The mean minimum breakage velocity approach was employed to capture the minimum impact energy triggering each glass breakage. The crack morphology of glass panels is firstly analyzed. It is followed by identifying the precise crack initiation and propagation features in the case where both glass panels break in the same impact attempt. The effects caused by three design variables on the impact resistance of LG panels were then examined. Several key conclusions can be made:

a) The intersection angle of the radial crack edges increases when the strengthening level of glass decreases. In the case that both glass panels break in the same impact, the inner glass panel cracks first with radial cracks more frequently, while the outer glass panel fracture will initiate after lagging for nearly 0.08 ms.
b) The glass make up with inner HS glass and outer FT glass panels can evidently improve the impact resistance, and performs better in keeping initial stiffness under repeated impacts with higher impact velocity. If HS glass is adopted in the both sides of glass panel, it may weaken the impact resistance.
c) When comparing with 3.04 mm interlayer, 1.52 mm PVB interlayer can provide better impact resistance and higher initial stiffness, it is also more likely to render the stiffness degradation between consecutive breakages.
d) Compared to PVB laminated glass, SGP laminated glass cannot achieve better impact resistance, but it presents remarkable higher initial pre breakage stiffness and remains greater post breakage strength.
e) The critical velocity (corresponding impactor mass is 13.5 kg) that leads to the nonlinearity of the P_{max}-V relationship in different breakage sequence is revealed.

Acknowledgements

This work was supported by the National Key Research and Development Program of China [Grant No. 2017YFC0806100], the Science Research Plan of Shanghai Municipal Science and Technology Committee [Grant No. 17DZ1200306] and the National Natural Science Foundation of China [Grants No. 51378308].

References

Acloque, P.: Déformation et rupture des verres. Ann Mines **2**, 57-66 (1975)
ASTM E1886-13a, Standard Test Method for Performance of Exterior Windows, Curtain Walls, Doors, and Impact Protective Systems Impacted by Missile(s) and Exposed to Cyclic Pressure Differentials. In. ASTM International, (2013)
ASTM E1996-14a, Standard Specification for Performance of Exterior Windows, Curtain Walls, Doors, and Impact Protective Systems Impacted by Windborne Debris in Hurricanes. In. ASTM International, (2014)
ASTM F3007-13, Standard Test Method for Ball Drop Impact Resistance of Laminated Architectural Flat Glass. In. ASTM International, (2013)
Bennison, S.J., Smith, C.A., Duser, A.V., Jagota, A.: Structural performance of laminated glass made with a "stiff" interlayer. In: The use of glass in buildings. ASTM International, (2002)
BS EN 356 - Glass in building. Security glazing. Testing and classification of resistance against manual attack. In. British Standards Institution, (2000)
Dugnani, R., Zednik, R.J., Verghese, P.: Analytical model of dynamic crack evolution in tempered and strengthened glass plates. International Journal of Fracture **190**(1-2), 75-86 (2014)
Grant, P.V., Cantwell, W.J., McKenzie, H., Corkhill, P.: The damage threshold of laminated glass structures. International Journal of Impact Engineering **21**(9), 737-746 (1998). doi:http://dx.doi.org/10.1016/S0734-743X(98)00027-X
Kaiser, N.D., Behr, R.A., Minor, J.E., Dharani, L.R., Ji, F., Kremer, P.A.: Impact Resistance of Laminated Glass Using "Sacrificial Ply" Design Concept. Journal of Architectural Engineering **6**(1), 24-34 (2000). doi:doi:10.1061/(ASCE)1076-0431(2000)6:1(24)
Knight, C.G., Swain, M.V., Chaudhri, M.M.: Impact of small steel spheres on glass surfaces. Journal of Materials Science **12**(8), 1573-1586 (1977). doi:10.1007/bf00542808
Liu, B., Xu, T., Xu, X., Wang, Y., Sun, Y., Li, Y.: Energy absorption mechanism of polyvinyl butyral laminated windshield subjected to head impact: Experiment and numerical simulations. International Journal of Impact Engineering **90**, 26-36 (2016). doi:https://doi.org/10.1016/j.ijimpeng.2015.11.010
Molnár, G., Ferentzi, M., Weltsch, Z., Szebényi, G., Borbás, L., Bojtár, I.: Fragmentation of wedge loaded tempered structural glass. Glass Structures & Engineering **1**(2), 385-394 (2016). doi:10.1007/s40940-016-0010-9
Nielsen, J.H., Olesen, J.F., Stang, H.: The Fracture Process of Tempered Soda-Lime-Silica Glass. Experimental Mechanics **49**(6), 855 (2008). doi:10.1007/s11340-008-9200-y
Pantelidesa, C.P., Horstb, A.D., Minorc, J.E.: Post-breakage behavior of architectural glazing in Windstorms. Journal of Wind Engineering & Industrial Aerodynamics **44**(1-3), 2425-2435 (1992)
Pyttel, T., Liebertz, H., Cai, J.: Failure criterion for laminated glass under impact loading and its application in finite element simulation. International Journal of Impact Engineering **38**(4), 252-263 (2011). doi:https://doi.org/10.1016/j.ijimpeng.2010.10.035
Rooij, L.V., Bhalla, K., Meissner, M., Ivarsson, J., Crandall, J., Longhitano, D., Takahashi, Y., Dokko, Y., Kikuchi, Y.: Pedestrian crash reconstruction using multi-body modeling with geometrically detailed, validated vehicle models and advanced pedestrian injury criteria. Paper presented at the 18th ESV Conference,
Saxe, T.J., Behr, R.A., Minor, J.E., Kremer, P.A., Dharani, L.R.: Effects of Missile Size and Glass Type on Impact Resistance of “Sacrificial Ply” Laminated Glass. Journal of Architectural Engineering **8**(1), 24-39 (2002)
Van Dam, S.: Experimental Analysis of the Post-Fracture Response of Laminated Glass under Impact and Blast Loading. Chent University (2017)
Zhang, X., Hao, H., Ma, G.: Laboratory test and numerical simulation of laminated glass window vulnerability to debris impact. International Journal of Impact Engineering **55**(5), 49-62 (2013)